Unidirectional hybrid silicon ring laser with an intracavity S-bend

Wesley D. Sacher,[1,*] Michael L. Davenport,[2] Martijn J. R. Heck,[2] Jared C. Mikkelsen,[1] Joyce K. S. Poon,[1] and John E. Bowers[2]

[1]*Department of Electrical and Computer Engineering, University of Toronto, 10 King's College Road, Toronto, Ontario, M5S 3G4, Canada*

[2]*Department of Electrical and Computer Engineering, University of California at Santa Barbara, Santa Barbara, California 93106, USA*

[*]*wesley.sacher@mail.utoronto.ca*

Abstract: We demonstrate a hybrid silicon ring laser with an internal amplifying S-bend that couples a fraction of the counter-clockwise circulating light into the the clockwise direction. The device supported single-mode, unidirectional laser oscillation at certain bias conditions. A spatial field distribution model is derived to describe the unidirectional operation. A unidirectional clockwise laser output with a suppression ratio up to 18.6 dB over the counter-clockwise mode was achieved.

OCIS codes: (250.5960) Semiconductor lasers; (250.5300) Photonic integrated circuits; (140.3560) Lasers, ring.

References and links

1. W. Bogaerts, P. De Heyn, T. Van Vaerenbergh, K. De Vos, S. Kumar Selvaraja, T. Claes, P. Dumon, P. Bienstman, D. Van Thourhout, and R. Baets, "Silicon microring resonators," Laser Photon. Rev. **6**, 47–73 (2012).
2. D. Liang and J. E. Bowers, "Recent progress in lasers on silicon," Nat. Photonics **4**, 511–517 (2010).
3. J. V. Campenhout, P. R. Romeo, P. Regreny, C. Seassal, D. V. Thourhout, S. Verstuyft, L. D. Cioccio, J.-M. Fedeli, C. Lagahe, and R. Baets, "Electrically pumped InP-based microdisk lasers integrated with a nanophotonic silicon-on-insulator waveguide circuit," Opt. Express **15**, 6744–6749 (2007).
4. G.-H. Duan, C. Jany, A. Le Liepvre, A. Accard, M. Lamponi, D. Make, P. Kaspar, G. Levaufre, N. Girard, F. Lelarge, J.-M. Fedeli, A. Descos, B. Ben Bakir, S. Messaoudene, D. Bordel, S. Menezo, G. de Valicourt, S. Keyvaninia, G. Roelkens, D. Van Thourhout, D. Thomson, F. Gardes, and G. Reed, "Hybrid III-V on silicon lasers for photonic integrated circuits on silicon," IEEE J. Sel. Top. Quantum Electron. **20**, 158–170 (2014).
5. P. Goldberg, P. W. Milonni, and B. Sundaram, "Theory of the fundamental laser linewidth," Phys. Rev. A **44**, 1969–1985 (1991).
6. M.-C. Wu, Y.-H. Lo, and S. Wang, "Linewidth broadening due to longitudinal spatial hole burning in a long distributed feedback laser," Appl. Phys. Lett. **52**, 1119–1121 (1988).
7. Y. Shoji, T. Mizumoto, H. Yokoi, I.-W. Hsieh, and R. M. Osgood, "Magneto-optical isolator with silicon waveguides fabricated by direct bonding," Appl. Phys. Lett. **92**, 071117 (2008).
8. M.-C. Tien, T. Mizumoto, P. Pintus, H. Kromer, and J. E. Bowers, "Silicon ring isolators with bonded nonreciprocal magneto-optic garnets," Opt. Express **19**, 11740–11745 (2011).
9. S. Ghosh, S. Keyvavinia, W. V. Roy, T. Mizumoto, G. Roelkens, and R. Baets, "Ce:YIG/Silicon-on-Insulator waveguide optical isolator realized by adhesive bonding," Opt. Express **20**, 1839–1848 (2012).
10. M. Kneissl, M. Teepe, N. Miyashita, N. M. Johnson, G. D. Chern, and R. K. Chang, "Current-injection spiral-shaped microcavity disk laser diodes with unidirectional emission," Appl. Phys. Lett. **84**, 2485–2487 (2004).
11. Q. J. Wang, C. Yan, N. Yu, J. Unterhinninghofen, J. Wiersig, C. Pflügl, L. Diehl, T. Edamura, M. Yamanishi, H. Kan, and F. Capasso, "Whispering-gallery mode resonators for highly unidirectional laser action," Proc. Natl. Acad. Sci. U.S.A. **107**, 22407–22412 (2010).
12. J. J. Liang, S. T. Lau, M. H. Leary, and J. M. Ballantyne, "Unidirectional operation of waveguide diode ring lasers," Appl. Phys. Lett. **70**, 1192–1194 (1997).

#241687 Received 28 May 2015; revised 18 Jul 2015; accepted 3 Sep 2015; published 30 Sep 2015

13. S. Oku, M. Okayasu, and M. Ikeda, "Control of unidirectional oscillation in semiconductor orbiter lasers," IEEE Photon. Technol. Lett. **3**, 1066–1068 (1991).
14. F. R. Faxvog, "Modes of a unidirectional ring laser," Opt. Lett. **5**, 285–287 (1980).
15. S. H. Cho and R. J. Ram, "High counter-mode suppression semiconductor ring lasers," in "Integrated Photonics Research," (Optical Society of America, 2002), p. IThC1.
16. D. Liang, S. Srinivasan, D. Fattal, M. Fiorentino, Z. Huang, D. Spencer, J. Bowers, and R. Beausoleil, "Teardrop reflector-assisted unidirectional hybrid silicon microring lasers," IEEE Photon. Technol. Lett. **24**, 1988–1990 (2012).
17. P. Mechet, S. Verstuyft, T. de Vries, T. Spuesens, P. Regreny, D. V. Thourhout, G. Roelkens, and G. Morthier, "Unidirectional III-V microdisk lasers heterogeneously integrated on SOI," Opt. Express **21**, 19339–19352 (2013).
18. J. P. Hohimer, G. A. Vawter, and D. C. Craft, "Unidirectional operation in a semiconductor ring diode laser," Appl. Phys. Lett. **62**, 1185–1187 (1993).
19. M. J. R. Heck, J. F. Bauters, M. L. Davenport, J. K. Doylend, S. Jain, G. Kurczveil, S. Srinivasan, Y. Tang, and J. E. Bowers, "Hybrid silicon photonic integrated circuit technology," IEEE J. Sel. Top. Quantum Electron. **19**, 6100117 (2013).
20. S. H. Cho and R. J. Ram, "Unidirectionality of semiconductor ring lasers: theory and experiment," in "IEEE 18th International Semiconductor Laser Conference," (2002), pp. 69–70.
21. D. Liang, A. Fang, H. Park, T. Reynolds, K. Warner, D. Oakley, and J. Bowers, "Low-temperature, strong SiO_2-SiO_2 covalent wafer bonding for III–V compound semiconductors-to-silicon photonic integrated circuits," J. Electron. Mater. **37**, 1552–1559 (2008).
22. G. Kurczveil, P. Pintus, M. Heck, J. Peters, and J. Bowers, "Characterization of insertion loss and back reflection in passive hybrid silicon tapers," IEEE Photon. J. **5**, 6600410 (2013).
23. M. Sorel, G. Giuliani, A. Scire, R. Miglierina, S. Donati, and P. Laybourn, "Operating regimes of GaAs-AlGaAs semiconductor ring lasers: experiment and model," IEEE J. Quant. Electron. **39**, 1187–1195 (2003).
24. L. Gelens, S. Beri, G. Van der Sande, G. Mezosi, M. Sorel, J. Danckaert, and G. Verschaffelt, "Exploring multistability in semiconductor ring lasers: Theory and experiment," Phys. Rev. Lett. **102**, 193904 (2009).
25. S. Lardenois, D. Pascal, L. Vivien, E. Cassan, S. Laval, R. Orobtchouk, M. Heitzmann, N. Bouzaida, and L. Mollard, "Low-loss submicrometer silicon-on-insulator rib waveguides and corner mirrors," Opt. Lett. **28**, 1150–1152 (2003).
26. R. Hanfoug, L. M. Augustin, Y. Barbarin, J. J. G. M. van der Tol, E. A. J. M. Bente, F. Karouta, D. Rogers, S. Cole, Y. S. Oei, X. J. M. Leijtens, and M. K. Smit, "Reduced reflections from multimode interference couplers," Electron. Lett. **42**, 465-466 (2006).

1. Introduction

Ring resonators are common in today's silicon (Si) and hybrid Si integrated photonics platforms, because their critical dimensions are amenable to the resolution of foundry fabrication processes using 193 nm or 248 nm deep ultraviolet lithography [1–4]. For ring lasers, it is often desirable to have only one sense of light circulation in the cavity for single-mode operation, to prevent emission of light into an undesired direction, and to eliminate spatial hole burning, which may reduce the laser noise and linewidth [5, 6]. Unidirectional ring lasers typically require a non-reciprocal loss element in the laser cavity, such as an optical isolator. While magneto-optic materials can be flip-chip bonded onto Si waveguides [7–9], the extra bonding step complicates the fabrication process of chip-scale ring lasers.

To achieve unidirectional emission in ring lasers without an isolator, several approaches have been proposed. Spiral geometries and whispering gallery mode resonators with notches in the periphery can have highly directional far-field emission patterns [10, 11]. Triangular and square shaped resonators can also be used [12, 13]. Another strategy is to couple a fraction of the power in the counter-clockwise (CCW) circulating mode into the clockwise (CW) circulating mode to preferentially enable CW laser emission. This coupling can be achieved either by an external reflector placed at the output port of the CCW mode [14–17], or by incorporating an amplifying S-bend into the ring cavity as in [15, 18]. In hybrid III-V-on-Si platforms, only unidirectional ring lasers that use an external reflector have been reported [16, 17], but the demonstrations did not include monitors to directly measure the ratio of the CCW and CW intracavity circulating powers. Compared to monolithic lasers, hybrid Si lasers potentially have added intracavity

#241687 Received 28 May 2015; revised 18 Jul 2015; accepted 3 Sep 2015; published 30 Sep 2015

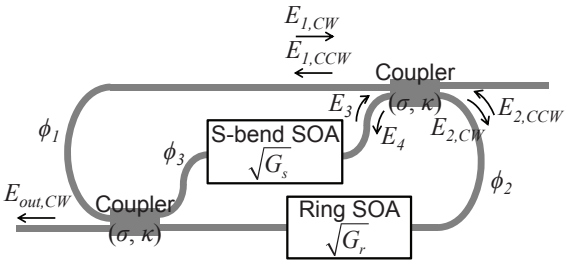

Fig. 1. Schematic of a ring laser with an integrated S-bend. The CW and CCW electric field amplitudes are labeled over arrows. The couplers have field through and cross-coupling coefficients of σ and κ, respectively. The field amplitude gains of the S-bend and ring SOAs are $\sqrt{G_s}$ and $\sqrt{G_r}$, respectively. The complex phase-shifts for the left and right halves of the ring, and the S-bend are ϕ_1, ϕ_2, and ϕ_3, respectively.

reflections due to the high index contrast of Si waveguides and the inter-layer transitions. Such intracavity reflections affect the unidirectional operation.

In this article, we study a hybrid III-V-on-Si ring laser with an integrated amplifying S-bend path capable of unidirectional operation. A spatially distributed steady-state analysis shows that the design can robustly lead to unidirectional laser oscillation. Our laser uses standard building blocks in the UCSB hybrid Si integrated photonics platform [19]. In contrast to [16, 17], here, the CW and CCW intracavity powers were directly compared to quantify the unidirectional operation using a power tap in the ring at the expense of added losses in the resonator.

2. Device geometry and analysis

The laser geometry based on [18] is illustrated in Fig. 1. The ring contains an S-bend and semiconductor optical amplifiers (SOAs) in the ring path and in the S-bend. The S-bend connects to the ring using two couplers, and it diverts a fraction of the CCW power and spontaneous emission generated in the S-bend into the CW mode. The CW mode remains in the ring and does not couple into the CCW mode. Although the round-trip losses experienced by the CW and CCW modes are identical (as all the elements in the ring resonator are reciprocal), the non-reciprocal injection of a fraction of the CCW circulating optical power into the CW mode leads to unidirectional laser emission. A rate equation analysis of this effect was presented in [20] for fiber ring lasers with SOAs. Here, we present an alternative analytical model of the laser.

In Fig. 1, the CW and CCW field amplitudes in the ring are $E_{1,CW}$, $E_{1,CCW}$, $E_{2,CW}$, and $E_{2,CCW}$, and the field amplitudes in the S-bend are E_3 and E_4. The main CW output is $E_{out,CW}$. We assume the two couplers that connect the S-bend to the ring have identical field through- and cross-coupling coefficients, σ and κ, respectively. For simplicity, we neglect spontaneous emission. The optical power gain of the main SOA in the ring is G_r and the gain of the SOA in the S-bend is G_s. We let ϕ_1, ϕ_2 and ϕ_3 be complex to represent the phase accumulation and field attenuation in the left part of the ring, the right part of the ring, and the S-bend, respectively. With these definitions, the field amplitudes are

$$E_{1,CW} = \kappa\sqrt{G_r}\mathrm{e}^{-i(\phi_1+\phi_2)}E_{2,CW} + \sigma\sqrt{G_s}\mathrm{e}^{-i(\phi_1+\phi_3)}E_4, \tag{1a}$$

$$E_{2,CW} = \kappa E_{1,CW} + \sigma E_3, \tag{1b}$$

$$E_{1,CCW} = \kappa E_{2,CCW}, \tag{1c}$$

$$E_{2,CCW} = \kappa\sqrt{G_r}\mathrm{e}^{-i(\phi_1+\phi_2)}E_{1,CCW}, \tag{1d}$$

#241687 Received 28 May 2015; revised 18 Jul 2015; accepted 3 Sep 2015; published 30 Sep 2015

$$E_3 = \sigma e^{-i(\phi_1+\phi_3)}\sqrt{G_s}E_{1,CCW}, \tag{1e}$$

$$E_4 = \sigma E_{2,CCW}, \tag{1f}$$

$$E_{out,CW} = \sigma\sqrt{G_r}e^{-i\phi_2}E_{2,CW} + \kappa\sqrt{G_s}e^{-i\phi_3}E_4. \tag{1g}$$

To include spontaneous emission, a small stochastic noise term can be added to the equations, which will lead to a fluctuating amplitude originating from each of the SOAs.

Substituting Eq. (1b) into Eq. (1a) and simplifying using Eqs. (1d)-(1f), we arrive at an expression for the unidirectionality factor, U, representing the ratio between the CW and CCW circulating optical powers:

$$U \equiv \left|\frac{E_{1,CW}}{E_{1,CCW}}\right|^2 = \frac{4|\kappa|^2|\sigma|^4 a_r a_s G_r G_s}{1+|\kappa|^4 a_r G_r - 2\sqrt{a_r G_r}|\kappa|^2\cos(2\theta_\kappa+\phi_r)}. \tag{2}$$

In the above, $\phi_r = \mathrm{Re}(\phi_1+\phi_2)$ is the round-trip phase-shift in the ring, θ_κ is the phase-shift of the coupler (i.e., $\kappa = |\kappa|e^{-i\theta_\kappa}$), $a_r = \left[\mathrm{Re}(e^{-i\phi_1-i\phi_2})\right]^2$ is the round-trip power attenuation in the ring, and $a_s = \left[\mathrm{Re}(e^{-i\phi_1-i\phi_3})\right]^2$ is the power attenuation of the path taken by the fraction of the CCW circulating amplitude, $E_{1,CCW}$, that is injected into the CW direction. U does not depend on the phase-shift in the S-bend because the two possible paths that divert $E_{1,CCW}$ into $E_{1,CW}$ have the same phase-shift.

From Eq. (2), we find that unidirectional CW laser emission occurs ($U \to \infty$) when the round-trip phase and gain conditions are satisfied as follows:

$$2\theta_\kappa + \phi_r = 2n\pi, \quad \text{where } n \text{ is an integer;} \tag{3a}$$

$$G_r = \frac{1}{|\kappa|^4 a_r}, \tag{3b}$$

which results in a denominator that is equal to zero. The laser condition in Eq. (3) is identical to that of a ring without the injection of CCW light into the CW mode via the S-bend. In other words, ideally, the laser is expected to be unidirectional when the threshold condition determined by the ring is met. Equation (2) also shows that unidirectional CCW laser emission is not possible because the numerator cannot equal zero. However, due to spontaneous emission, U is finite in practice. At a given value of G_r (i.e., at a given pump current applied to the ring SOA and a given optical output power), Eq. (2) predicts that the unidirectionality increases linearly with the gain of the SOA in the S-bend at a given wavelength. Thus, U would increase roughly linearly at low injection currents and low optical intensities, but would decrease as G_s is reduced, e.g., due to gain saturation or compression.

Finally, from Eq. (1g), the main CW output, $E_{out,CW}$, is the superposition of the fields exiting the ring and the S-bend. Therefore, if the laser is not strongly unidirectional, the interference leads to a complicated dependence of the output power on the relative phase between the ring and S-bend paths. This interference may be controlled using phase-shifters in the ring and S-bend paths. Alternatively, to avoid this interference, a power tap in the ring path can be used for the laser output instead of the couplers at the junctions in the two end of the S-bend. The laser output at the power tap would simply be proportional to the intracavity CW power.

The above model is meant to highlight the mechanism behind the unidirectional behavior, and the model's simplicity (e.g., neglect of small intracavity reflections) prevents accurate fitting to the experimental data in Section 4.

#241687 Received 28 May 2015; revised 18 Jul 2015; accepted 3 Sep 2015; published 30 Sep 2015

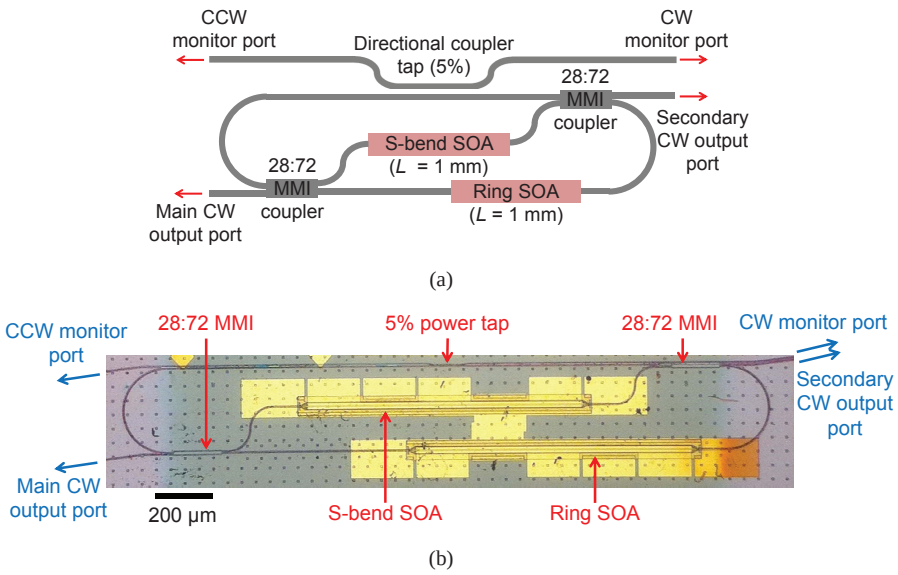

Fig. 2. (a) Schematic and (b) annotated optical micrograph of the fabricated hybrid Si laser with an integrated amplifying S-bend. The CW monitor port and secondary CW output port are adjacent and difficult to distinguish in the micrograph.

3. Fabricated device

The device was implemented in the UCSB hybrid Si integrated photonics platform [19], and a schematic and optical micrograph of the device are shown in Fig. 2. To monitor the CW and CCW intracavity light, we incorporated a 5% directional coupler tap into the ring. Two 28:72 multimode interference (MMI) couplers (i.e., with 72% cross-coupled power coefficient) were used to incorporate the S-bend into the ring. Si rib waveguides were formed in a silicon-on-insulator substrate with a 500 nm thick top Si layer, a 250 nm thick partially-etched Si slab, and a 1 μm thick buried oxide layer. Cleaved III-V dies were wafer-bonded onto the Si using a low temperature hydrophilic bonding process [21] and reactive ion etching was used to define the SOAs. Pd/Ge/Pd/Au and Pd/Ti/Pd/Au contacts were deposited to form the N and P contacts, respectively. The laser operated in the transverse-electric polarization, and adiabatic tapers in the III-V and Si layers were used to transition the Si rib waveguide mode into the hybrid mode of the SOA regions [22]. The ring and S-bend SOA lengths were 1 mm long, the Si rib waveguide loss was about 8 dB/cm, the loss per transition was about 0.8 dB, and the reflection from each transition was about -29 dB. To reduce the reflections at the facets, the output waveguides were tilted at an angle of 7^{o} relative to the polished facets, and the facets were coated with a two-layer anti-reflection coating for a -33 dB power reflection per facet.

4. Measurements

The die was mounted on a temperature-controlled stage set at 20^{o}C, and light was collected from the output ports using lensed single-mode fibers with a nominal spot diameter of 2.5 μm at 1550 nm. The unidirectionality factor was extracted from fiber-coupled optical power measurements at the CW and CCW monitor ports. Throughout the measurements, we optimized for the fiber-to-chip alignment using the waveguide path between the two monitor ports. By assuming the fiber-to-chip coupling losses were identical at the two monitor ports and calibrating for the

#241687 Received 28 May 2015; revised 18 Jul 2015; accepted 3 Sep 2015; published 30 Sep 2015

fiber-to-chip coupling loss, we extracted the on-chip optical power at the main CW output port.

Figures 3(a) and (b) show the on-chip optical power at the main CW output port and the unidirectionality factor as a function of the ring and S-bend SOA currents. The S-bend and ring SOA currents were stepped in increments of 5 mA and 10 mA, respectively. For greater clarity, Figs. 3(c) and (d) show a few vertical slices of the data. U tended to increase with the S-bend SOA current, confirming the analysis in Section 2. When the S-bend SOA current was $\lesssim 55$ mA, U was generally low (between about 0.3 and 3), since the S-bend path was effectively removed. The laser output power did not increase linearly with the ring SOA current, especially when the S-bend current increased. This is likely due to the combined effects of the interference in Eq. (1g), multi longitudinal mode oscillation, and minute intracavity reflections. Intracavity reflections cause parasitic power coupling from the CW mode to the CCW mode, which can result in multistability [23, 24]. The reflections could be from the MMI couplers, sidewall roughness, and transitions between the Si waveguides and SOAs. The plot of the sum of the on-chip powers at the CW and CCW monitor ports vs. ring SOA current in Fig. 3(e) exhibits kinks that are suggestive of multimode oscillation and the presence of intracavity reflections.

The highest value of U measured was 72 or 18.6 dB, when the S-bend SOA current was 137.5 mA and the ring SOA current was 112.5 mA. This value is not captured in the coarse sweep in Fig. 3(b). Figure 4(a) shows the main CW output power and U at a S-bend SOA current of 137.5 mA as a function of the ring SOA current. The output power and unidirectional operation were sensitive to the current applied to the ring SOA. The CW and CCW monitor port powers in Fig. 4(b) show that the intracavity CW power is maximized when U is maximized ($U = 72$). The main CW output spectrum when $U = 72$ is shown in Fig. 4(c). Interestingly, at

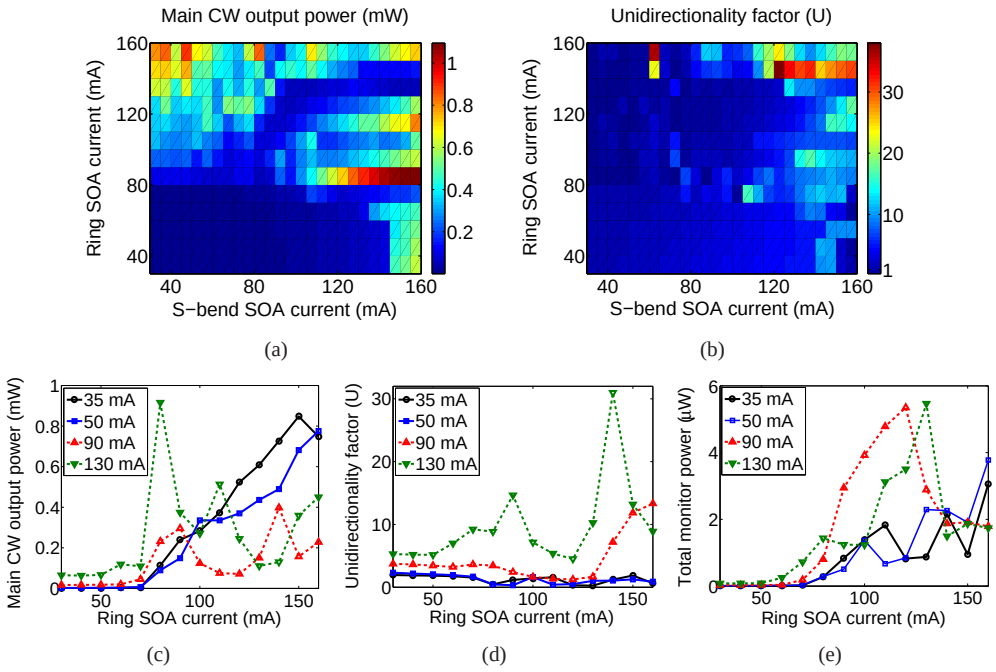

Fig. 3. (a) On-chip main CW output power and (b) U as a function of the ring and S-bend SOA currents. (c) On-chip main CW output power, (d) U, and (e) sum of on-chip CW and CCW monitor port powers vs. the ring SOA current at various S-bend SOA currents. (c) and (d) are vertical slices of (a) and (b), respectively.

#241687 Received 28 May 2015; revised 18 Jul 2015; accepted 3 Sep 2015; published 30 Sep 2015

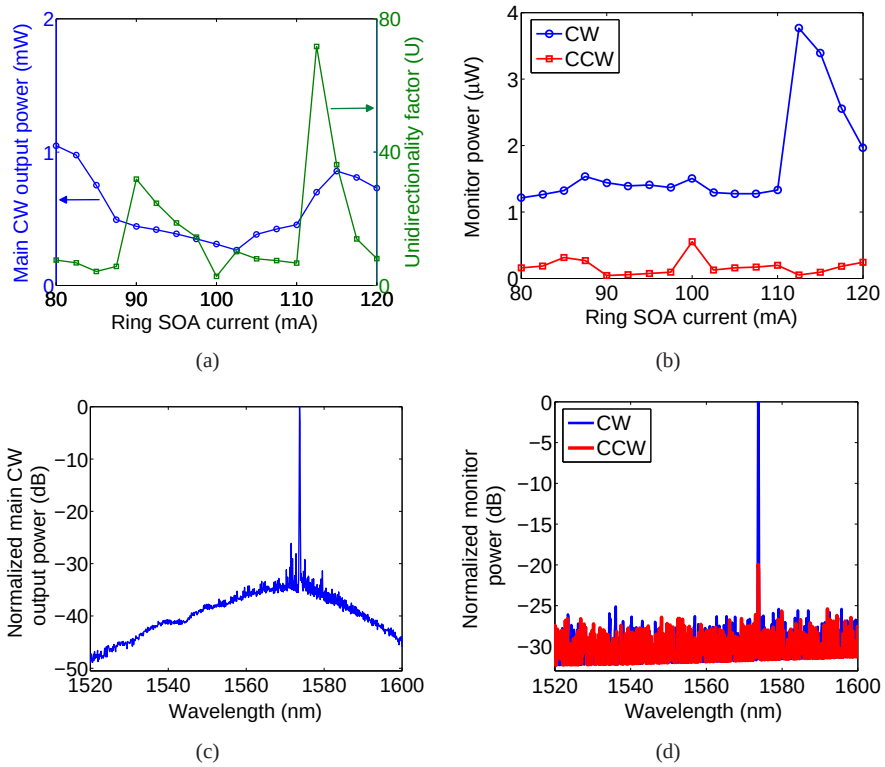

Fig. 4. (a) On-chip main CW output power and U vs. ring SOA current for an S-bend SOA current of 137.5 mA. (b) On-chip CW and CCW monitor port powers vs. ring SOA current for an S-bend SOA current of 137.5 mA. (c) Spectrum of the main CW output at the maximum U operating point. (d) Spectra of the CW and CCW monitor ports at the maximum U point.

this maximal value of U, the laser emission appeared to be single-mode up to the resolution of the optical spectrum analyzer of 0.1 nm. Furthermore, in Fig. 4(d), the CW and CCW monitor port spectra for the maximum U value show that the intracavity CW and CCW fields are both single-mode with the same wavelength. This mode selectivity provides further evidence for the impact of reflections within the cavity on the complex behaviour of the laser output power and unidirectional operation. Additional spectra were measured at lower U values between 1 and 34; some operating points were single-mode while others were multi-mode, and no simple dependence of the side-mode suppression ratio on U could be identified.

The output power and stability limitations of the laser can be overcome through straightforward optimization approaches. First, the output power can be improved by reducing the cavity losses. By reducing the 8 dB/cm Si waveguide loss to 1 dB/cm, as in [25], the ring path losses can be reduced by about 2.7 dB. Second, reducing intracavity reflections can improve the stability for high unidirectionality over a wider range of SOA currents. Importantly, the MMI couplers have not been optimized for low reflection, and by appropriate angling of the MMI interfaces the reflections could be greatly reduced as in [26].

#241687 Received 28 May 2015; revised 18 Jul 2015; accepted 3 Sep 2015; published 30 Sep 2015

5. Conclusions

We have demonstrated the unidirectional operation of a hybrid Si ring laser with an internal amplifying S-bend. A suppression of the CCW power relative to the CW power up to 18.6 dB and single-mode operation was observed. A drawback of the device was the sensitivity of the unidirectionality and output power to the SOA currents. Devices with reduced intracavity reflections and losses will improve the unidirectionality and output power.

Acknowledgments

The authors are grateful for the support from DARPA through the EPHI program and from NSERC through the Discovery and Canada Research Chairs programs.

#241687 Received 28 May 2015; revised 18 Jul 2015; accepted 3 Sep 2015; published 30 Sep 2015